Two-energy-gap preformed-pair scenario for cuprate superconductors: Implications for angle-resolved photoemission spectroscopy

Chih-Chun Chien,[1] Yan He,[1] Qijin Chen,[2,1] and K. Levin[1]
[1]*Department of Physics and James Franck Institute, University of Chicago, Chicago, Illinois 60637, USA*
[2]*Department of Physics and Zhejiang Institute of Modern Physics, Zhejiang University, Hangzhou, Zhejiang 310027, China*
(Received 15 April 2009; published 25 June 2009)

We show how, within a preformed-pair scenario for the cuprate pseudogap, the nodal and antinodal responses in angle-resolved photoemission spectroscopy necessarily have very different temperature T dependences. We examine the behavior and the contrasting T dependences for a range of temperatures both below and above T_c. Previously, the distinct nodal and antinodal responses have provided strong support for the "two-gap scenario" of the cuprates in which the pseudogap competes with superconductivity. Instead, our theory supports a picture in which the pseudogap derives from pairing correlations, identifying the two-gap components with noncondensed and condensed pairs. Our calculations are based on a microscopic diagrammatic approach for addressing pairing correlations in a regime where the attraction is stronger than BCS and the coherence length is anomalously short. This many body theory-based scheme takes as a starting point the BCS ansatz for the ground-state wave function and incorporates finite temperature effects through coupled equations for the single particle and pair propagators (or T matrix). It leads to reasonably good agreement with a range of different photoemission measurements in the moderately underdoped regime and we emphasize that here there is no explicit curve fitting. We briefly address the more heavily underdoped regime in which the behavior is more complex.

DOI: 10.1103/PhysRevB.79.214527 PACS number(s): 74.20.−z, 74.25.Jb, 74.72.Hs, 79.60.−i

I. INTRODUCTION

A. Background literature

An important dichotomy is emerging in descriptions of the mysterious pseudogap phase of the cuprates which has resulted in different theoretical scenarios.[1] At the heart of this dispute is whether the pseudogap observed in the normal state is derived from the superconductivity itself or whether it results from a competing, but somewhat elusive order parameter. Experiments (i) which directly study this anomalous normal phase have provided evidence for both points of view.[2–5] However, there is an even larger class of recent experiments (ii) which address the superconducting phase. These are based on angle-resolved photoemission[6–8] and Raman scattering[9,10] as well as scanning tunneling microscopy.[11–14] They quite generally reveal that there are two distinct temperature dependences associated with the behavior of the spectral function and related properties in the nodal and antinodal regions of momentum space. The nodal response appears to reflect superconducting order whereas the antinodal response is much less sensitive to T_c. For this reason, it is speculated that the pseudogap may derive from a competing order parameter. Finally, there is a third class of experiments (iii) which probe the behavior as the system evolves from above to just below T_c and establish that the transition is clearly second order. Here, for example, one sees a very smooth evolution of the angle-resolved photoemission spectroscopy (ARPES) response in the antinodal direction.[15,16] Many other properties[17,18] which depend on the excitation gap show no clear signature of T_c. This is generally interpreted as evidence in favor of a precursor-superconductivity origin to the pseudogap.

It is the last two classes of experiments which are the focus of this paper. Indeed, there is very little in the theoretical literature which addresses these phenomena. Rather the emphasis has been on the ground state or on the normal, pseudogap phase. Our goal is to show how to reconcile, in particular, the experiments of class (ii) with a preformed-pair scenario. Moreover, it is possible that the arguments presented here can be viewed as "modular" in the sense of applying to alternate precursor-superconductivity approaches such as the "phase fluctuation" approach[19] or the resonant valence bond (RVB) scheme.[20] We stress that there appear to be no counterpart studies of the intermediate temperature broken symmetry state within the more widely espoused phase fluctuation scheme.[19] Our explanation of the dichotomy is built around a picture in which the short coherence length cuprates are somewhere between BCS and Bose-Einstein condensed (BEC) systems. This crossover scheme seems to be gaining in support[1,21] and is now widely studied in the cold Fermi gases.[17,22,23] Our emphasis here is on moderately underdoped cuprates where at the lowest temperatures the spectral properties appear to conform to that of a simple d-wave BCS-like state.[7,24] While the behavior appears to be much more complex in the heavily underdoped regime, nevertheless, there is a smooth evolution with doping and all the indications for distinct nodal and antinodal responses are present at moderate underdoping. Thus, we feel the same qualitative physics regarding the origin of the pseudogap is appropriate to both moderately and heavily underdoped cuprates.

We build on a d-wave BCS-like ground state where the variational parameters are determined in conjunction with a self-consistency condition for the chemical potential, μ. This self-consistent treatment of μ (which is close to but different from E_F) is necessary[25,26] to accommodate the relatively short coherence length of the cuprates. Our contribution in the past[17,27] has been to address the associated finite tempera-

ture behavior within a microscopic, diagram-based T-matrix theory. In earlier papers the anomalous behavior of the Nernst coefficient and of the optical conductivity were also addressed within this framework,[28,29] along with other experiments,[17] including[30] the nature of the specific-heat jump and the behavior of the conductance dI/dV. Moreover, a number of years ago[30] we presented a description of the spectral function with special emphasis on how superconducting coherence would be evident in the presence of a normal state pseudogap. A central point of the present paper is to show that these calculations (which predate the actual experiments[7,24] by five years or more), yield very good semiquantitative agreement with a wide range of more recent ARPES experiments without invoking any fitting parameters or phenomenology.

At the onset, we present the simple physical picture of the different ARPES spectral gap responses as a function of **k**. We note that the nodal regions are associated with extended gapless states or Fermi arcs[24] which are now rather reasonably well understood[31] within a preformed-pair scenario above T_c. Their collapse below T_c has also been addressed within the present formalism.[32] One can anticipate (as we find) that the arcs are sensitive to the onset of the order parameter, which we call Δ_{sc}, in the same way that a strict BCS superconductor (which necessarily has a gapless normal state) is acutely sensitive to the onset of ordering. By contrast, the antinodal points are not as affected by passing through T_c because they already possess a substantial pairing gap in the normal phase. One will also reach this conclusion by arguing that it is a corollary of a second order transition. If there is a difference between the nodal and antinodal responses above T_c (as is implicit in the presence of the Fermi arcs), it must persist, as we find here, for some range of temperatures below T_c. A key point to implementing this physical picture is the realization that the excitation gap which we call Δ is, at all temperatures (except strictly $T=0$), different from the order parameter Δ_{sc}. This distinction trivially holds in the normal, pseudogap phase.

B. Physical picture of BCS-BEC crossover scenario

Before presenting our microscopic scheme it is useful to sketch a simple physically intuitive approach of the BCS-BEC crossover scenario at finite temperatures. This approach should be seen to be distinct from the phase fluctuation scenario. As shown in Fig. 1 the precursor superconductivity here refers literally to preformed-pairs, rather than (as in the phase fluctuation scheme)[19] to extended regions or grains where the order-parameter amplitude is well established while the phase is uncorrelated. These preformed-pairs arise from a stronger than BCS attraction. This strong attraction breaks the usual degeneracy between Δ and Δ_{sc} or the similar degeneracy between the pair formation temperature T^* and condensation temperature T_c. Within this BCS-BEC scenario, the mechanism for pairing need not be specified. The physics focuses on the anomalously short coherence length of the cuprates (associated with strong attraction or high T^*), whereas in the phase fluctuation scenario the focus is on the anomalously low plasma frequency–leading to soft

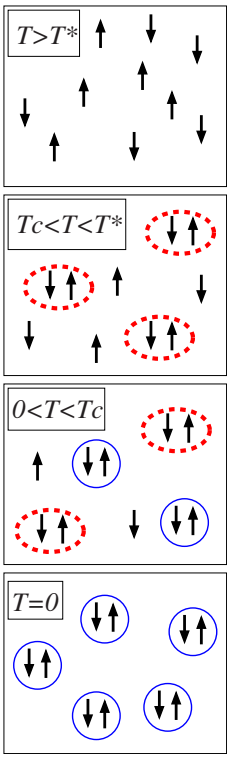

FIG. 1. (Color online) Cartoon of the model showing noncondensed pairs in (red) open ellipses, and condensed pairs in (blue) closed circles. The number of noncondensed pairs scales with the height of the shaded region in the following figure.

phase fluctuations and more mesoscopic regions of superconductivity.

Figure 1 shows the schematic behavior as one passes from above T^* to the fully condensed ground state. The (red) dotted lines enclose Cooper pairs with net finite momentum, while the (blue) solid pairs correspond to the components of the condensate which are at zero center of mass momentum and have phase coherence. The third panel with $0<T<T_c$ is the most interesting from the perspective of the present paper. This is the regime about which there has been very little theoretical discussion in the literature and this is the regime where the interesting two-gap scenario physics is emerging. Here one sees a three-way coexistence of the condensate, the fermionic excitations (denoted by a single spin arrow), and of pair excitations or noncondensed pairs. When there is a stronger than BCS attractive interaction, preformed-pairs above T_c, which are responsible for the pseudogap, do not disappear but rather evolve smoothly below T_c into this unusual form of condensate excitation arising from noncondensed pairs. This leads to two-gap contributions[33] in the superfluid phase representing the finite momentum pair excitations of the condensate (associated with the component, Δ_{pg}) and the condensed pairs (associated with the order parameter, Δ_{sc}).

In this two-gap preformed-pair scenario there is a gradual interconversion of noncondensed to condensed pairs as the temperature decreases. This is shown in Fig. 2 where the energy gap parameters are schematically plotted. Above T_c but below T^* the excitation gap reflects the fact that one has

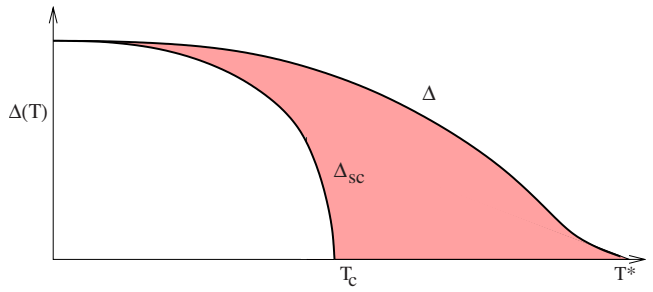

FIG. 2. (Color online) Contrasting behavior of the excitation gap $\Delta(T)$ and superfluid order parameter $\Delta_{sc}(T)$ versus temperature. The number of noncondensed pairs varies as $\Delta_{pg}^2=\Delta^2-\Delta_{sc}^2$.

to add energy in order to create fermionic excitations or break pairs. This excitation gap Δ smoothly evolves below T_c as in a second-order phase transition, while precisely at T_c the order parameter Δ_{sc} opens up. The difference between the (squares) of these two parameters can be associated with the number of noncondensed pairs. Figure 2 thus shows that the number of noncondensed pairs is finite below T_c provided the temperature is different from zero. We will show, using our microscopic scheme that the two-gap components add in quadrature[33] to yield the square of the thermodynamical gap parameter $\Delta(T)$. Importantly, $\Delta(T)$ is essentially temperature independent as a consequence of this interconversion from $\Delta_{pg}(T)$ to $\Delta_{sc}(T)$. Just as there are two-gap parameters, there are two temperature scales: T^* marking the gradual onset of the pseudogap, as well as T_c which marks the appearance of the condensate.

How do we understand the phase diagram of the cuprates within the BCS-BEC crossover approach? Our interest here is not on the details of the hole concentration dependence although this has been discussed elsewhere.[22,34] There is a pronounced competition between T^* and T_c within the BCS-BEC crossover scenario as the attractive interaction $|U|$ increases.[35] Indeed, when T^* increases (as for example with underdoping) T_c will ultimately decrease. This is due to the fact that at large $|U|$, it is energetically very expensive to unbind a pair of fermions as is required in the pair hopping process. A large effective pair mass is then responsible for a small T_c. In the d-wave case[17] this pair hopping is even more restricted because of the extended size of the pair, which leads to pair localization, and quite possibly the "singlet glass" phase which has been reported recently.[13] Importantly, this concomitant cessation of T_c occurs while the system is still deep in the fermionic regime where the chemical potential μ is positive, suggesting a phase diagram not so different from that of the cuprates.[22,36]

II. OVERVIEW OF FULLY MICROSCOPIC THEORY

Having discussed the simple physical picture we next review in more detail the underlying microscopic (T matrix) theoretical formalism, which leads to it.[17,30,36]

A. T-matrix theory

We begin with a BCS-like ground state: $\Psi_0=\Pi_{\mathbf{k}}(u_{\mathbf{k}}+v_{\mathbf{k}}c_{k,\uparrow}^{\dagger}c_{-k,\downarrow}^{\dagger})|0\rangle$, where the parameters $u_{\mathbf{k}}$ and $v_{\mathbf{k}}$ are determined variationally in conjunction with a self-consistent condition for the chemical potential, μ. Knowing, as we now do, that at the lowest temperatures the spectral properties appear to conform to that of simple BCS-like d-wave pairing serves to justify this starting point. We have extensively addressed the finite temperature behavior associated with this fully condensed ground state as well as the spectral properties.[30]

To address d-wave pairing in the cuprates we need to incorporate specific $\mathbf{k}$ dependent factors so that the gap parameters in the self-energy acquire the form $\Delta_{\mathbf{k},sc}=\Delta_{sc}\varphi_{\mathbf{k}}$ and $\Delta_{\mathbf{k},pg}=\Delta_{pg}\varphi_{\mathbf{k}}$, where we introduce $\varphi_{\mathbf{k}}=\cos(2\phi)$, to reflect the d-wave $\mathbf{k}$ dependence along the Fermi surface. We adopt a tight binding model for the band dispersion $\epsilon_{\mathbf{k}}=2t(2-\cos k_x-\cos k_y)+2t_z(1-\cos k_z)+4t'(1-\cos k_x\cos k_y)$. It should be stressed that all gap parameters have the same $\mathbf{k}$ dependence. Additional effects of anisotropy (beyond those in $\varphi_{\mathbf{k}}$), which appear in the measured spectral gaps, are not presumed to be present in the initial gap parameters.

We will next briefly summarize the key equations which emerge from our T- matrix scheme.[17,27] Throughout this paper, we adopt a four-vector notation: $Q\equiv(i\Omega_l,\mathbf{q})$, $K\equiv(i\omega_n,\mathbf{k})$, $\Sigma_Q\equiv T\Sigma_l\Sigma_{\mathbf{q}}$, and $\Sigma_K\equiv T\Sigma_n\Sigma_{\mathbf{k}}$, where ω_n and Ω_l are the odd and even Matsubara frequencies, respectively. We also take $\hbar=k_B=1$. Within the present approach there are two contributions to the full T-matrix

$$t=t_{pg}+t_{sc} \tag{1}$$

where

$$t_{sc}(Q)=-\frac{\Delta_{sc}^2}{T}\delta(Q). \tag{2}$$

Similarly, we have two terms for the fermion self-energy

$$\Sigma(K)=\Sigma_{sc}(K)+\Sigma_{pg}(K)=\sum_Q t(Q)G_0(Q-K)\varphi_{\mathbf{k}-\mathbf{q}/2}^2, \tag{3}$$

where G_0 is the bare Green's function. It follows then that

$$\Sigma_{sc}(\mathbf{k},i\omega_n)=\frac{\Delta_{\mathbf{k},sc}^2}{i\omega_n+\epsilon_{\mathbf{k}}-\mu}=\frac{\Delta_{\mathbf{k},sc}^2}{i\omega_n+\xi_{\mathbf{k}}}. \tag{4}$$

Here $\xi_{\mathbf{k}}=\epsilon_{\mathbf{k}}-\mu$. Throughout, the label pg corresponds to the "pseudogap" and the corresponding noncondensed pair propagator is given by

$$t_{pg}(Q)=\frac{U}{1+U\chi(Q)}, \tag{5}$$

where the pair susceptibility $\chi(Q)$ has to be properly chosen to arrive at the BCS-Leggett ground state and U is the attractive pairing interaction. We impose the natural BEC condition that below T_c there is a vanishing chemical potential for the noncondensed pairs

$$\mu_{\text{pair}}=0, \tag{6}$$

which means that $t_{pg}(Q)$ diverges at $Q=0$ when $T\leq T_c$. Thus, we approximate[33,37] $\Sigma_{pg}(K)$ to yield

$$\Sigma_{pg}(K)\approx -G_0(-K)\Delta_{\mathbf{k},pg}^2,\quad (T\leq T_c), \tag{7}$$

with

$$\Delta_{pg}^2 \equiv -\sum_{Q\neq 0} t_{pg}(Q). \tag{8}$$

It follows that we have the usual BCS-like form for the self-energy

$$\Sigma(\mathbf{k}, i\omega_n) \approx \frac{\Delta_{\mathbf{k}}^2}{i\omega_n + \xi_{\mathbf{k}}}, \quad (T \leq T_c) \tag{9}$$

with $\Delta_{\mathbf{k}} = \Delta\varphi_{\mathbf{k}}$ and

$$\Delta^2(T) = \Delta_{pg}^2(T) + \Delta_{sc}^2(T). \tag{10}$$

As is consistent with the standard ground-state constraints, Δ_{pg} vanishes at $T \equiv 0$, where all pairs are condensed.

Using this self-energy, one determines G and thereby can evaluate t_{pg}. Then the condition that the noncondensed pairs have a gapless excitation spectrum ($\mu_{\text{pair}}=0$) becomes the usual BCS gap equation, except that it is the excitation gap Δ and not the order parameter Δ_{sc} which appears here. We then have from Eq. (6)

$$1 + U\sum_{\mathbf{k}} \frac{1-2f(E_{\mathbf{k}})}{2E_{\mathbf{k}}}\varphi_{\mathbf{k}}^2 = 0, \quad T \leq T_c, \tag{11}$$

where $E_{\mathbf{k}} = \sqrt{\xi_{\mathbf{k}}^2 + \Delta_{\mathbf{k}}^2}$ is the quasiparticle dispersion.

To close the loop, for consistency we take for the pair susceptibility

$$\chi(Q) = \sum_K G_0(Q-K)G(K)\varphi_{\mathbf{k}-\mathbf{q}/2}^2. \tag{12}$$

Here $G = (G_0^{-1} - \Sigma)^{-1}$ is the full Green's function. Similarly, using

$$n = 2\sum_K G(K) \tag{13}$$

one derives

$$n = \sum_{\mathbf{k}} \left[1 - \frac{\xi_{\mathbf{k}}}{E_{\mathbf{k}}} + 2\frac{\xi_{\mathbf{k}}}{E_{\mathbf{k}}} f(E_{\mathbf{k}}) \right], \tag{14}$$

which is the natural generalization of the BCS number equation. The final set of equations which must be solved is rather simple and given by Eqs. (8), (11), and (14). Note that in the normal state (where μ_{pair} is nonzero), Eq. (7) is no longer a good approximation, although a natural extension can be readily written down.[38]

To evaluate Δ_{pg}^2 in Eq. (8) we note that at small four-vector Q, we may expand the inverse of t_{pg} after analytical continuation. Because we are interested in the moderate and strong coupling cases, where the contribution of the quadratic term in Ω term is small, we drop this term and thus find the following expression, which, after analytical continuation, yields the expansion

$$t_{pg}(Q) = \frac{1}{Z(\Omega - \Omega_q^0 + \mu_{\text{pair}}) + i\Gamma_Q}, \tag{15}$$

where $\Omega_{\mathbf{q}}^0 = q^2/(2M^*)$ and where Z is the inverse residue given by

$$Z = \left.\frac{\partial t_{pg}^{-1}}{\partial\Omega}\right|_{\Omega=0,q=0} = \frac{1}{2\Delta^2}\left[n - 2\sum_{\mathbf{k}} f(\xi_{\mathbf{k}}) \right]. \tag{16}$$

We note that the q^2 dispersion in $t_{pg}(Q)$ means that for a range of low T, Δ_{pg}^2 will vary as $T^{3/2}$. Below T_c the imaginary contribution in Eq. (15) $\Gamma_Q \to 0$ faster than q^2 as $q \to 0$. It should be stressed that this approach yields the ground-state equations and that it represents a physically meaningful extension of this ground state to finite T. We emphasize that the approximation in Eq. (7) is not central to the physics, but it does greatly simplify the numerical analysis.

B. Detailed behavior of the self-energy

We have seen that, after analytical continuation, the self-energy is given by $\Sigma(\mathbf{k},\omega) = \Sigma_{sc}(\mathbf{k},\omega) + \Sigma_{pg}(\mathbf{k},\omega)$, where

$$\Sigma(\mathbf{k},\omega) = \frac{\Delta_{\mathbf{k},sc}^2}{\omega + \xi_{\mathbf{k}}} + \Sigma_{pg}(\mathbf{k},\omega) \tag{17}$$

$$\approx \frac{\Delta_{\mathbf{k},sc}^2}{\omega + \xi_{\mathbf{k}}} + \frac{\Delta_{\mathbf{k},pg}^2}{\omega + \xi_{\mathbf{k}}} \tag{18}$$

The BCS-Leggett ground-state equations[26] follow. In invoking the approximation contained in Eq. (7), we are in effect ignoring the difference between condensed and noncondensed pairs which cannot be strictly correct. The simplest correction to Σ_{pg} (which should apply above and below T_c) is to write an improved form which most importantly accommodates the fact that the coherent Cooper pairs of the condensate are infinitely long lived, whereas the incoherent or noncondensed pairs have a finite inverse lifetime γ

$$\Sigma_{pg}(\mathbf{k},\omega) \approx \frac{\Delta_{\mathbf{k},pg}^2}{\omega + \xi_{\mathbf{k}} + i\gamma} + \tilde{\Sigma}(\mathbf{k},\omega). \tag{19}$$

Here $\tilde{\Sigma}(\mathbf{k},\omega)$ represents the lifetime associated with channels other than the pairing channel and, as is conventional, we parameterize $\tilde{\Sigma}(\mathbf{k},\omega) \equiv -i\Sigma_0$. Thus we have

$$\Sigma(\mathbf{k},\omega) = \left(\frac{\Delta_{\mathbf{k},pg}^2}{\omega + \xi_{\mathbf{k}} + i\gamma} - i\Sigma_0 \right) + \frac{\Delta_{\mathbf{k},sc}^2}{\omega + \xi_{\mathbf{k}}}. \tag{20}$$

The above equation contains a well-known form for Σ_{pg}. It also contains the important addition of Σ_{sc}. The model for Σ_{pg} was determined in the present context on the basis of detailed numerical studies[30,39] and has been deduced independently[40] and widely applied.[31] in the cuprate literature. Here the broadening $\gamma \neq 0$ and "incoherent" background contribution Σ_0 reflect the fact that noncondensed pairs do not lead to *true* off-diagonal long-range order. While we can think of γ as a phenomenological parameter in the spirit of the literature[31,41] we stress that there is a microscopic basis for considering this broadened BCS form.[37,42] The precise value of γ and its T dependence are not particularly important for the present purposes, as long as it is nonzero at finite T. By contrast Σ_{sc} is associated with long-lived condensed Cooper pairs and is similar to Σ_{pg} but without the broadening. It is, moreover, often assumed that $-i\Sigma_0 \approx -i\gamma$, although this assumption is not necessary.

C. Spectral function and superfluid density

The resulting spectral function, based on Eqs. (17) and (19) is given by

$$A(\mathbf{k},\omega)=\frac{2\Delta_{pg,\mathbf{k}}^2\gamma(\omega+\xi_{\mathbf{k}})^2}{(\omega+\xi_{\mathbf{k}})^2(\omega^2-E_{\mathbf{k}}^2)^2+\gamma^2(\omega^2-\xi_{\mathbf{k}}^2-\Delta_{sc,\mathbf{k}}^2)^2}. \tag{21}$$

For convenience, here we do not show the effects of the Σ_0 term. Above T_c, Eq. (21) is used with $\Delta_{sc}=0$. It can be seen that at all $\mathbf{k}$ and below T_c, this spectral function contains a zero at $\omega=-\xi_{\mathbf{k}}$, whereas it has no zero above T_c. This means that a clear signature of phase coherence is present when one passes from above to below T_c, as long as $\gamma\neq 0$ distinguishes the noncondensed from the condensed pairs.

These dramatic effects of the condensate in the spectral function are also important for addressing the specific-heat jump at T_c which must be present as a thermodynamic indication of the phase transition. The onset of a condensate below T_c (with no lifetime broadening, $\gamma=0$) in contrast to the lifetime broadened contribution from the pseudogap is associated with clear signatures in the specific heat[30] as the system develops superconducting coherence.

Physically, one can anticipate that the noncondensed pairs represent an additional mechanism for destroying the condensate. It is important to stress that as a consequence this approach is different from a Fermi liquid-based superconductor which has often been presumed in the theoretical literature.[9] Because the normal state is, by consensus, a non-Fermi liquid, and because there is a smooth evolution from above to below T_c, it should not appear surprising that the superconducting phase is also nonFermi liquid-based. Important to the analysis of the superfluid density is the imposition of gauge invariance through a Ward identity. In this way one finds[36,43] that the pseudogap contributions via Σ_{pg} to the superfluid density precisely cancel in contrast to those from Δ_{sc}.

After this cancellation, the superfluid density is found to be of the simple form[36]

$$\left[\frac{n_s(T)}{m}\right]=\left[1-\frac{\Delta_{pg}^2(T)}{\Delta^2(T)}\right]\left\{\frac{n_s[T,\Delta(T)]}{m}\right\}^{\mathrm{BCS}}. \tag{22}$$

Here, importantly, the quantity $(n_s(T,\Delta(T))/m)^{\mathrm{BCS}}$ corresponds to the conventional BCS form for the d-wave superfluid density, albeit with an unusual essentially T-independent gap $\Delta(T)$ in the underdoped regime. In summary, one sees that n_s is additionally depressed by *bosonic fluctuations* which ensure that n_s vanishes at T_c, not T^*.

D. Abbreviated model

To make the present formalism more widely accessible we construct a simplified or abbreviated model in which T^* and T_c are effectively fit to the cuprate phase diagram and the various gap parameters Δ_{pg} and Δ_{sc} which appear in the spectral function are then readily deduced. For the purposes of the present paper we do not focus on this short cut scheme, but it serves to make the results here easily reproducible by others.

We have seen that in the temperature regime below or only slightly above T_c, the thermodynamical energy gap $\Delta(T)$ and its component $\Delta_{pg}(T)$ satisfies $\Delta^2(T)=\Delta_{pg}^2(T)+\Delta_{sc}^2(T)$ where we define $E_{\mathbf{k}}^{2d}\equiv\sqrt{(\xi_{\mathbf{k}}^{2d})^2+\Delta_{\mathbf{k}}^2}$ and presume that $\Delta(T)\equiv\Delta_{mf}(T)$ satisfies the (two-dimensional mean field) BCS gap equation

$$0=1+U\sum_{\mathbf{k}}\frac{1-2f(E_{\mathbf{k}}^{2d})}{2E_{\mathbf{k}}^{2d}}\varphi_{\mathbf{k}}^2,\quad\text{with} \tag{23}$$

$$\Delta_{pg}^2(T)\approx(T/T_c)^{3/2}\Delta^2(T_c),\quad T\leq T_c,$$

$$=\Delta^2(T),\quad T\geq T_c. \tag{24}$$

Here the superscript $2d$ refers to the fact that we drop the third dimension in the energy dispersion so that $t_z\to 0$. At each x, the parameter U is chosen to yield the measured T^* and, knowing T_c, $\Delta(T_c)$ can be determined. These equations must be solved in conjunction with a self-consistent particle number equation for μ. Lying behind this phenomenological approach is the fact that in a fully consistent theory,[34] T_c is (logarithmically) dependent on the interlayer hopping t_z and it vanishes when this parameter is absent where the system is strictly two dimensional. Thus we can view t_z as a fitting parameter which depends on hole concentration x. In the fully self-consistent scheme one recovers the entire cuprate phase diagram for $T^*(x)$ and $T_c(x)$ by a proper choice of $U(x)$ and $t_z(x)$. The short cut scheme then allows one to calculate without too much effort, the various gap parameters as a function of temperature and x which appear in the spectral function.

We see that because the total gap $\Delta(T,x)$ satisfies the BCS equation there is a BCS relation between T^* and $\Delta(T=0)$. In this way Eq. (23) implies that the excitation gap Δ contains the energy scale T^*, not T_c. Indeed, at intermediate values of the attractive interaction $|U|$, $\Delta(T)$ is essentially independent of temperature from the ground state (where $\Delta_{pg}=0$) to well above T_c. We will not discuss the hole concentration dependence x in detail in this paper, because it has been treated elsewhere.[32,36] Finally, we note that within this BCS-BEC scenario, the mechanism for pairing need not be specified. Nevertheless, it is clear that the increase in T^* with decreasing x requires that the attractive pairing interaction must become stronger as the Mott-insulator phase is approached.

III. NUMERICAL RESULTS

A. General properties of the spectral functions

We turn now to detailed numerical calculations of the behavior of the spectral function, $A(\phi,\omega)$ on the Fermi surface (where $\epsilon_{\mathbf{k}}-\mu=0$). Throughout we will define the spectral (or ARPES) gap as one half the peak to peak separation in the spectral function (when it exists). The dispersion $\epsilon_{\mathbf{k}}$ is obtained using our two-dimensional tight-binding model. For the most part we will consider a prototypical hole concentration $x=0.125$, which is associated with a particular value of U in Eq. (11) leading to $T_c/T^*\approx 0.5$. We choose a bandwidth of $4t=250$ meV and this results in a $T=0$ gap about 34 meV.

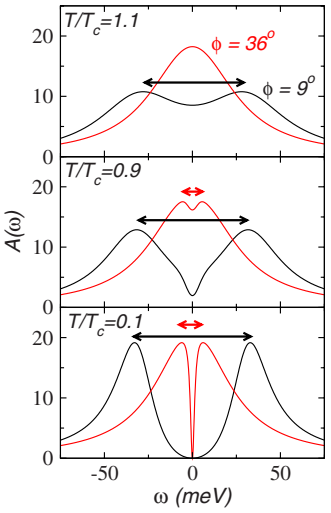

FIG. 3. (Color online) Spectral function $A(\phi,\omega)$ at $T/T_c=1.1,0.9,0.1$ (from top to bottom) for $\phi=9°$ (black) and $\phi=36°$ (red). Black and red arrows indicate size of the spectral gap, which is measured in ARPES.

Our results are insensitive to the specific parameter set as we will demonstrate below. The only constraint to be imposed from experiment is that there must be sizeable Fermi arcs (of order, say, 10° out of 45°) in the normal phase for a moderately underdoped sample. This means that the parameter γ at T_c is not much less than about one half Δ at the same temperature. The parameter Σ_0 is found to be relatively unimportant for the purposes of the plots we present here. It is reasonable to presume that the lifetime associated with the noncondensed pairs increases as temperature is lowered, since their number becomes fewer. For definiteness, following Ref. 32, we take $\Sigma_0=26$ meV independent of T and $\gamma=26$ meV at 95 K with $\gamma(T)=\gamma(95\ \mathrm{K})(T/95\ \mathrm{K})$ above T_c and $\gamma=\gamma(T_c)(T/T_c)^3$ below T_c. To be more consistent with experimental data, when spectral functions are presented we convolve the spectral function with a Gaussian instrumental broadening curve with a standard deviation $\sigma=3$ meV.

Figure 3 illustrates the temperature evolution of the spectral function for $\phi=9°$ (close to the antinodes) and $\phi=36°$ (close to the nodes) at $T/T_c=1.1,0.9,0.1$ from top to bottom. Above T_c (top panel) the well-understood behavior[31,32] sets the stage for the normal phase which underlies the superconducting state in the next two panels. In this top panel, one sees Fermi arcs, which derive from the broadening term γ in Σ_{pg}, in the near-nodal direction and a pseudogap in the spectral function associated with Δ_{pg} near the antinodes. These arcs appear over that range of $\mathbf{k}$ values for which γ is larger than the momentum dependent pseudogap. When T is slightly below T_c (middle panel), a dip in the spectral function at $\phi=36°$ suddenly appears at $\omega=0$. At this ϕ the underlying normal state is gapless so that the onset of the additional component of the self-energy via Σ_{sc} with long-lived pairs ($\gamma=0$) leads to the opening of a spectral gap.

By contrast, the presence of this order parameter is not responsible for the gap near the antinodes ($\phi=9°$), which, instead, mostly derives from Δ_{pg}. Here the positions of the two maxima are relatively unchanged from their counterparts in the normal phase. However, Δ_{sc} does introduce a sharpening of the spectral function associated with the deepening of the dip at $\omega=0$. This can be seen analytically from Eq. (21) by noting that Σ_{sc} suppresses $A(\omega)$ near $\omega=0$. When $T\ll T_c$ (lower panel), pairing fluctuations are small so that $\Delta(T)\approx\Delta_{sc}(T)$ and one returns to a conventional BCS-like spectral function with well established gaps at all angles except at the precise nodes.

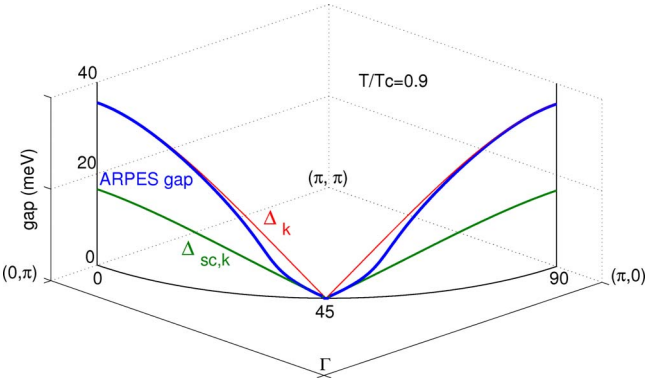

FIG. 4. (Color online) ARPES gap, $\Delta_{\mathbf{k}}$, and $\Delta_{\mathbf{k},sc}$ (labeled next to the corresponding curves) as a function of ϕ at $T/T_c=0.9$.

It is useful to look at the behavior of the ARPES gap over the entire range of ϕ as studied experimentally.[7] To emphasize that the spectral gap does not precisely correspond to the self-energy gap components, in Fig. 4 we plot the spectral function gap along with Δ, and Δ_{sc} as a function of angle at $T/T_c=0.9$. The figure illustrates that, near the antinodes, the spectral gap reflects the magnitude of Δ. Near the nodes, however, the spectral gap is more directly associated with Δ_{sc} in the sense that this gap appears only in the ordered phase. The second of these observations is in line with previous experimental findings.[6,8] However, it has generally been assumed that at the antinodes the behavior is governed by the so-called "pseudogap." We stress that our interpretation is not at odds with this literature. Rather we refer to the full gap at the antinodes as $\Delta(T)$ which is roughly a constant in temperature. This contains two contributions, one from $\Delta_{pg}(T)$ and one from the order parameter $\Delta_{sc}(T)$. While near T_c the former dominates, near $T\approx 0$, the latter is the more important. Thus the gap at the antinodes reflects superconducting order as well, at least in these moderately underdoped cuprates.

Figure 5 shows that the spectral gap shown by the blue lines in the previous figure for $T/T_c=0.9$ is only very slightly modified when the parameters Σ_0 (in the top panel) and γ (in the bottom panel) are altered. While the height of the peaks in the spectral function plots will be affected, the important derived quantities such as the spectral gap plotted in the figure are not changed when Σ_0 is varied by two orders of magnitude. Moreover, if γ is reasonably constrained to yield a sizeable Fermi arc above T_c, then the behavior of the spectral gap below T_c does not depend on the detailed values for γ.

B. Comparison between theory and experiment

Recently there has been an emphasis on experiments which contrast the behavior around the gap nodes with that

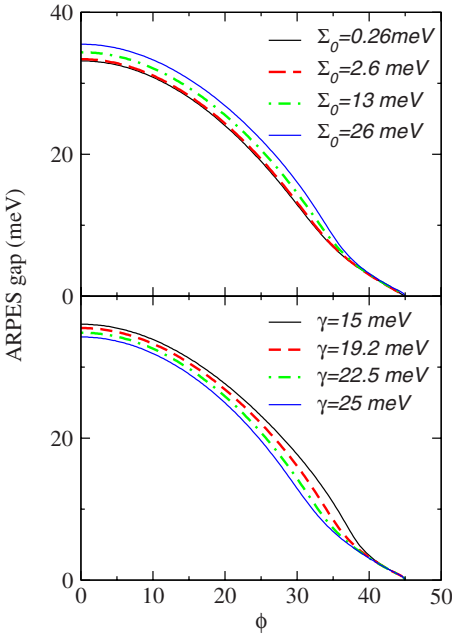

FIG. 5. (Color online) Parameter insensitivity. This is illustrated for $T/T_c=0.9$. Here we restricted γ to produce appropriately large arcs in the normal phase. Within this range there is virtually no change in the size of the deduced spectral gap. We explore two orders of magnitude variation in Σ_0 and again find no change in the spectral gap size.

around the gap maxima (or antinodes). The right panel of Fig. 6 indicates the size of the ARPES or spectral gap as deduced from one half of the peak to peak separation in the spectral function. These data[7] address a moderately underdoped sample. The three different curves correspond to three different temperatures with the legend the same as that in the left panel (representing the results of the present theory.) Importantly, one sees a pronounced temperature dependence in the behavior of the ARPES spectral gap for the nodal region (near 45°), as compared with the antinodal region (near 0 and 90°), where there is virtually no T dependence.

Theory (on the left) and experiment (on the right) are in reasonable agreement and one can readily understand the contrasting temperature response associated with the different $\mathbf{k}$ points on the Fermi surface. To see this, note that the nodal regions reflect extended gapless states or Fermi arcs[24] above T_c. It is natural to expect that they are sensitive to the onset of Δ_{sc}, in the same way that a strict BCS superconductor (which necessarily has a gapless normal state) is acutely sensitive to the presence of order. By contrast, the antinodal points are not as affected by passing through T_c because they already possess a substantial pairing gap in the normal phase.

The dramatic variation in the temperature dependence of the spectral gap as one moves along the Fermi surface has given rise to the so-called two-gap scenario.[1] In (perhaps) overly simplistic terms the one-gap and two-gap scenarios are differentiated by the presumption that in the former the pseudogap represents a precursor to superconductivity, while in the latter the mysterious cuprate pseudogap is viewed as arising from a competing order parameter. The two-gap scenario is viewed as a consequence of a number of different experiments[1,13] all of which have been interpreted to suggest that the antinodal region is associated with this alternative (hidden) order-parameter pseudogap and the nodal region is dominated by superconductivity. By contrast the viewpoint expressed here (based on BCS-BEC crossover theory) leads naturally to a different T dependence for the nodal and antinodal region, but at the same time it belongs to the class of theories which argue that the pseudogap is intimately connected with the superconductivity.

We turn in Fig. 7 to very important temperature dependent studies[7] which suggest that the nodal gap may directly reflect the order parameter. Figure 7(a) plots the various gap parameters, $\Delta(T)$, $\Delta_{pg}(T)$, and $\Delta_{sc}(T)$ in the self-energy as compared with the spectral gap measured near the node at $\phi=36°$ (indicated by squares) as a function of temperature. It can be seen that this spectral gap, while it is distinct from the order parameter $\Delta_{sc}(T)$ (except at the lowest temperatures), vanishes rather close to T_c. The figure shows that the gap parameter $\Delta(T)$ is relatively constant through T_c, so that the decrease in $\Delta_{pg}(T)$ with decreasing T is compensated by the increase in $\Delta_{sc}(T)$ through the interconversion of noncondensed and condensed pairs. To compare directly with experiment, in Fig. 7(b) we plot the spectral gap for two different angles, ϕ, as a function of T, in a fashion which looks rather similar to Fig. 2(d) of Ref. 7. For $\phi=30°$, which is somewhat further from the nodes there is a small spectral gap (pseudogap) above T_c. Because of the $\varphi_{\mathbf{k}}$ factor, closer to the antinodes the overall magnitude of the ARPES gap is larger than at $\phi=36°$.

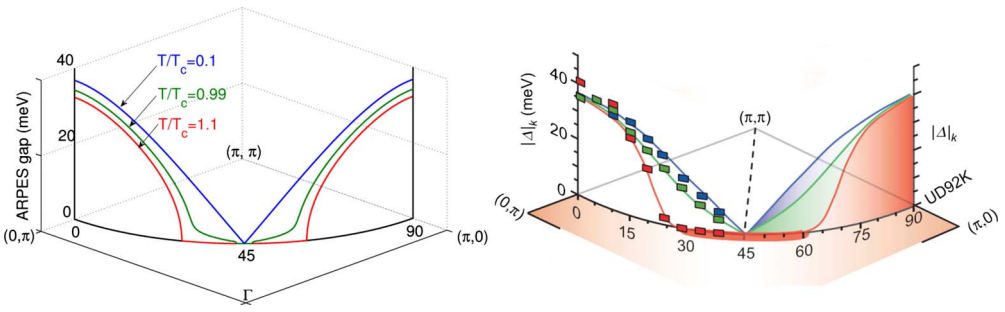

FIG. 6. (Color online) Contrasting nodal and antinodal temperature dependences in the d-wave case. Figure on the left is the ARPES gap as a function of angle ϕ at $T/T_c=1.1, 0.99, 0.1$ (labeled on the figure). This figure should be compared with the experimental plots on the right taken from Fig. 4b in Ref. 7

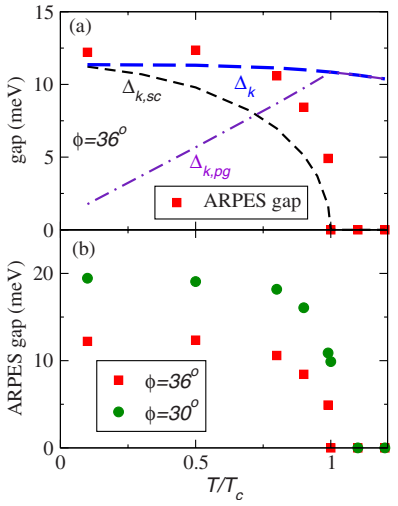

FIG. 7. (Color online) (a) The ARPES gap (red squares), $\Delta_{\mathbf{k}}$ (thick blue dashed line), $\Delta_{\mathbf{k},sc}$ (black dashed line), and $\Delta_{\mathbf{k},pg}$ (orange dot-dash line) as a function of T/T_c for $\phi=36°$. (b) The ARPES gap as a function of T/T_c for $\phi=36°$ (red squares) and $\phi=30°$ (green circles). This panel should be compared with Fig. 2d of Ref. 7.

In Fig. 8 we address the important issues which have been raised in Refs. 2, 7, and 24. These papers make the case that the pseudogap is a consequence of the superconductivity. The figure in the main body is a plot of the spectral gap for a few different temperatures from above to below T_c as a function of the simplest d-wave form for $\varphi_{\mathbf{k}}$. This figure compares favorably with Fig. 3(b) in Ref. 7. The central point illustrated here is that at the lowest temperatures one reverts, in effect, to a simple one-gap scenario. That is, the BCS-like ground-state wave function obtains with $\Delta=\Delta_{sc}$.

In the inset of Fig. 8 we present a contour plot of the occupied spectral weight corresponding to the product of the spectral function and Fermi function. In this way one can infer the dispersion relationship associated with the normal phase and see to what extent it is related to that below T_c. The left panel is below T_c and the right panel above T_c. This contour plot, albeit represented differently, compares rather favorably with Fig. 4 in Ref. 2. The similarity of the two panels would not be expected if the pseudogap were related to another order parameter.

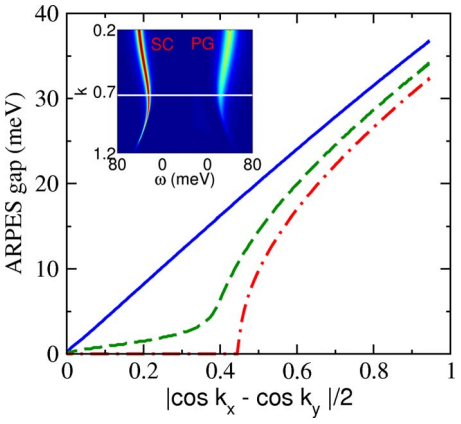

FIG. 8. (Color online) The ARPES gap as a function of $|\cos(k_x)-\cos(k_y)|/2$ for $T/T_c=0.1$ (blue solid line), 0.99 (green dashed line), and 1.1 (red dot-dash line). This should be compared with Fig. 3b of Ref. 7. Inset is a contour plot of the occupied spectral weight at $\phi=22.5°$, showing peak sharpening below T_c. We follow a similar sweep as that in Ref. 2 and the white line indicates the intersection with the Fermi surface. Here the intensity corresponding to below (left panel) and above (right) T_c is largest (smallest) in the red (blue) and we have taken smaller γ for illustrative purposes.

Together Fig. 8 and related experiments[2,7,24] provide evidence that the pseudogap has to be viewed as ultimately associated with the superconductivity. The normal-state excitations appear to have a (broadened) BCS-like dispersion. The nodal and antinodal behavior appear to be intimately connected in the ground state.

IV. PHENOMENOLOGICAL MODEL FOR HEAVILY UNDERDOPED SYSTEM

There is a growing body of work on more heavily underdoped cuprates[6,8,13] from which one can infer that the simple d wave, BCS-like ground state may not be appropriate nearer to the insulating phase. Here, if one looks at the experimental analog of Fig. 8, the lowest-temperature behavior still exhibits a deviation from the simple $\cos k_x - \cos k_y$ form. Indeed kinks are often seen[8] somewhat like that shown in Fig. 8, but for the case of very low temperatures. The kinks are associated with the fact that the ARPES gap curves in the nodal region seem to reflect the superconducting order while as before the antinodal behavior reflects what is referred to as the pseudogap. As a result it has been argued that[8] "the very different properties of these two gaps lead us to conclude that there is no direct relationship between the pseudogap and the superconducting gap".

Because there appears to be a rather continuous[7] evolution from moderate to heavy underdoping, we, instead speculate that the physics of the pseudogap in the two regimes must be rather similar and that the nonsimple d-wave ARPES gap behavior at the lowest temperatures in heavily underdoped cuprates is a natural extension of the higher $T<T_c$ behavior seen at moderate underdoping. At these higher $T<T_c$ there are two-gap components $\Delta_{pg}\neq 0$ and $\Delta_{sc}\neq 0$. Thus, a reasonable precursor-superconductivity-based phenomenological model for this extreme underdoped regime is to presume that Δ_{pg} persists into the ground state, perhaps because of a contamination from the nearby insulating phase. We view this insulating state as introducing a finite value for the zero-temperature pseudogap. This is consistent with the way[34] the insulating phase appears in our calculations where the pg gap component persists to the lowest temperatures while Δ_{sc} is strictly zero beyond a critical value for the attractive interaction or equivalently a critical value for T^*.

We emphasize that all previous discussions and figures have been microscopically based and derived, but in this section we proceed purely phenomenologically. The goal of this discussion is to arrive at a model for the extreme underdoped case which is smoothly connected to the physical picture we have thus far exploited for more moderately doped cuprates. We need to incorporate (i) a clear deviation from the d-wave ground state, (ii) kinks or other breaks in the

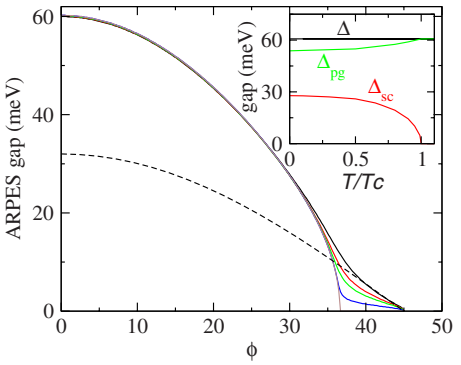

FIG. 9. (Color online) Behavior of the spectral gap as a function of angle ϕ for a phenomenological model representing a heavily underdoped system. The inset plots the gap functions which should be contrasted with that shown in Fig. 7(a). The dashed line is the extrapolation of the simple $\cos(2\phi)$ behavior found near the gap nodes. Solid curves from top to bottom correspond to $T/T_c = 0.1, 0.8, 0.9, 0.99, 1.1$.

ARPES gap function which distinguish different gap shapes around the nodal and antinodal regimes, and (iii) clear evidence for incoherence even below T_c, but only near the antinodes. The model we present grew out of a discussion with A. Yazdani and his collaborators[44] who have observed a similar gap shape in their scanning tunnel microscope experiments.

To describe this class of models we assume that all gap functions (but not the spectral gaps themselves) have the form $\Delta_{pg,\mathbf{k}} = \Delta_{pg}\varphi_{\mathbf{k}}$ and $\Delta_{sc,\mathbf{k}} = \Delta_{sc}\varphi_{\mathbf{k}}$. At a given temperature, the pseudogap now has two contributions: one from the usual preformed-pairs, which will ultimately go into the condensate at sufficiently low T and another from the admixture of insulating state which we view as a "zero-temperature pseudogap." In this way there is a weak-temperature dependence in Δ_{pg} associated with the pair-conversion process and concomitantly Δ_{sc} is also T dependent. A typical parameter set is shown in the inset of Fig. 9. This plot is to be contrasted with the behavior shown in Fig. 7(a).

For definiteness we presume that the total excitation gap is given by the mean-field gap $\Delta_{mf}(T)$ defined in Eq. (23), so that the superconducting order parameter contribution is $\Delta_{sc}(T) = \sqrt{\Delta_{mf}^2(T) - \Delta_{pg}^2(T)}$. The pseudogap contribution is written as $\Delta_{pg}(T) = \sqrt{\Delta_{pg0}^2(T) + \Delta_{pg1}^2(T)}$ with the zero temperature pseudogap given by $\Delta_{pg0}(T) = \alpha\Delta_{mf}(T)$ and $\Delta_{pg1}(T) = (T/T_c)^{3/2}\sqrt{\Delta_{mf}^2(T) - \Delta_{pg0}^2(T)}$ for $T \leq T_c$ and $\Delta_{pg}(T) = \Delta_{mf}(T)$ for $T > T_c$. Here $\Delta_{mf}(T)$ is the gap obtained from a mean-field calculation of d-wave BCS theory as derived from Eq. (23). In our microscopic calculations one would have $\alpha = 0$ which appears consistent with moderately underdoped systems. However, for heavily underdoped cuprates We choose α such that the sc and pg contributions at $T = 0$ are in the ratio of 1:2 as a typical example. We take $\gamma(T) = \Sigma_0(T) = 0.5\Delta_{pg}(T)$ for $T \leq T_c$ and $\gamma(T) = \Sigma_0(T) = (T/T_c)\gamma(T_c)$ for $T > T_c$.

Figure 9 shows the behavior of the spectral gap for the heavily underdoped model and for a range of temperatures $T/T_c = 0.1, 0.8, 0.9, 0.99, 1.1$. The dashed line is an extrapolation of the simple d-wave fitted form found near the gap nodes and associated with the order parameter Δ_{sc} at the lowest temperature. While there is a simple d-wave fitted form also at the antinodes the effective gap here is the much larger parameter Δ, which consists mostly of a pseudogap contribution, for this heavily underdoped system.

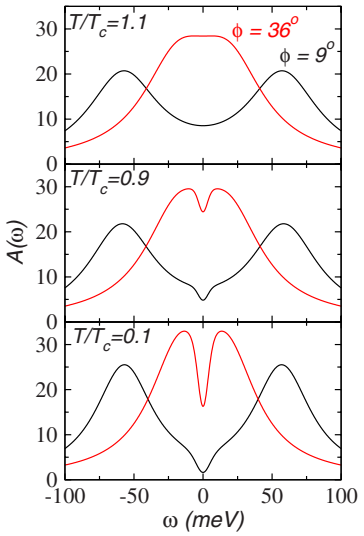

FIG. 10. (Color online) Spectral functions with convolution for phenomenological model of a heavily underdoped system. This model should show that at the lowest T the behavior around the antinodes is not much more coherent than that in the normal state. This figure should be contrasted with Fig. 3.

Figure 10 shows a plot of the actual spectral functions at two angles $\phi = 36°$ in red and $\phi = 9°$ in black at three different temperatures from above to just below T_c to finally at $T/T_c = 0.1$. The behavior in this heavily underdoped system can be contrasted with that shown in Fig. 3 for moderate doping. The nodal curves show the Fermi-arc behavior above T_c, followed by the opening of a gap (which reflects superconductivity) below T_c and the ultimate establishment of well-defined coherence with decreased T as evident by the narrow, well-defined peaks. By contrast the antinodal regime (unlike its counterpart in Fig. 3) does not indicate the presence of coherent quasiparticles. Rather, even at the lowest temperatures the peaks are broad and very little changed from those above T_c.

There are features of this model which do not capture all the phenomena observed experimentally. The "kink" effects seem to be strictly associated with the Fermi arcs of the normal state and not particularly close to the magnetic-zone boundary,[6] since the arc size is rather small in this underdoped regime. Moreover we have presumed a strictly d-wave gap shape which constrains the behavior of the spectral gap near the antinodes. Nevertheless, this is a reasonable model for further study, since it does preserve some of the key physics of the experiments.

V. CONCLUSIONS AND COMPARISONS WITH THE LITERATURE

This paper addresses issues which are at the center of major debates in high-temperature superconductivity. Do the

recent (so-called two-gap) experiments which report a difference associated with the nodal and antinodal response in ARPES[6–8] or in Raman,[9,10] or scanning tunneling microscopy[13,14] rule out the possibility that the pseudogap derives from the superconductivity itself? We argue that despite strong claims in the literature, pseudogap formation owing to preformed-pairs is, in fact, consistent with these experiments. We stress that our approach for the moderately underdoped cuprates is *not phenomenological*. It was in place well[30] before these experiments were undertaken.

We have emphasized that our explanation for the physics is relatively simple and is based on a stronger than BCS attractive interaction associated with short coherence length Cooper pairs. The formation of isolated pairs (in contrast to extended regions of fixed pairing amplitude) takes place at T^*, while condensation appears at T_c. What is crucial is that pseudogap effects which are associated with these preformed-pairs do not disappear immediately below T_c. Rather they persist as noncondensed pair excitations of the condensate. This is not a Fermi liquid-based form of superconductivity because there are bosonic degrees of freedom associated with the fermion pairs. Nor should this be thought of as a "one gap" picture. There are two components to the pairing gap, one from the noncondensed pairs and another from the condensate.

A central equation is Eq. (20) which shows that both components are important in the self-energy and therefore in the spectral function. The contribution from the preformed-pairs Σ_{pg} is crucial for forming the Fermi arcs above T_c. These appear in the nodal regions where γ is relatively larger than the momentum dependent gap. The contribution from the condensate Σ_{sc} is crucial just below T_c because it opens up a true gap in the Fermi-arc region. This is reminiscent of a conventional BCS superconductor which necessarily has a gapless normal state and is, thus, extremely sensitive to the presence of coherent order. This is, in contrast to the antinodal regimes where the large pseudogap above T_c is very little affected by the addition of the superconducting order, except through peak sharpening or coherence effects.

In the context of Eq. (20) it is generally believed[31] that there is only one component to the self-energy (Σ_{pg}) and that the onset of coherence coincides with a dramatic decrease in γ below T_c. We strongly disagree with this assumption. Rather there are two contributions to the self-energy below T_c and only one above. Thus, one should not argue that γ precisely vanishes at T_c but rather there is a continuous conversion from noncondensed to condensed pairs as T is lowered within the superfluid phase. The noncondensed pairs below T_c have finite lifetime while the condensed pairs do not.

In this paper we noted that there is additional experimental support for the fact that the pseudogap and the superconducting gap are intimately connected.[2,7,24] The lowest-temperature spectral properties[7,24] of, at least, moderately underdoped samples seem to fit a simple *d*-wave angular dependence and recent normal-state data[2] provide evidence for a dispersion deduced from the spectral function which is similar to that in the superfluid phase.

Finally, we addressed heavily underdoped cuprates in a phenomenological fashion. Here the simple *d*-wave gap shape may not be appropriate.[8] We argued that what is crucial is that there is a continuous evolution from moderate to extreme underdoping[7] so that it is unlikely that the pseudogap has a different origin in the two regimes. Rather some of the same physics must be at play. We postulated that there may be a zero temperature pseudogap present in highly underdoped systems which may derive from some admixture of the insulating phase.

In summary, this paper has shown how to reconcile a wide class of experiments in the moderately underdoped cuprates within a preformed-pair framework where there are, nevertheless, two components to the energy gap. This framework[33,36] predates the class of experiments we address here.

ACKNOWLEDGMENTS

This work was supported by NSF under Grant No. PHY-0555325 and NSF-MRSEC under Grant No. DMR-0213745. We thank S. Davis, A. Yazdani, Colin Parker, and Aakash Pushp, as well as Wei-Sheng Lee and D. Morr for helpful discussions.

[1] S. Hufner, M. A. Hossain, A. Damascelli, and G. Sawatzky, Rep. Prog. Phys. **71**, 062501 (2008).
[2] A. Kanigel, U. Chatterjee, M. Randeria, M. R. Norman, G. Koren, K. Kadowaki, and J. C. Campuzano, Phys. Rev. Lett. **101**, 137002 (2008).
[3] J. L. Tallon and J. W. Loram, Physica C **349**, 53 (2001).
[4] A. Kaminski, S. Rosenkranz, H. Fretwell, J. C. Campuzano, Z. Li, H. Raffy, W. G. Cullen, H. You, C. G. Olson, C. M. Varma, and H. Höchst, Nature (London) **416**, 610 (2002).
[5] S. V. Borisenko, A. A. Kordyuk, A. Koitzsch, T. K. Kim, K. A. Nenkov, M. Knupfer, J. Fink, C. Grazioli, S. Turchini, and H. Berger, Phys. Rev. Lett. **92**, 207001 (2004).
[6] K. Tanaka, W. S. Lee, D. H. Lu, A. Fujimori, T. Fujii, ' Risdiana, I. Terasaki, D. J. Scalapino, T. P. Devereaux, Z. Hussain, and Z. X. Shen, Science **314**, 1910 (2006).
[7] W. S. Lee, I. M. Vishik, K. Tanaka, D. H. Lu, T. Sasagawa, N. Nagaosa, T. P. Devereaux, Z. Hussain, and Z. X. Shen, Nature (London) **450**, 81 (2007).
[8] T. Kondo, R. Khasanov, T. Takeuchi, J. Schmalian, and A. Kaminski, Nature (London) **457**, 296 (2009).
[9] M. Le Tacon, A. Sacuto, A. Georges, G. Kotliar, Y. Gallais, D. Colson, and A. Forget, Nat. Phys. **2**, 537 (2006).
[10] W. Guyard, A. Sacuto, M. Cazayous, Y. Gallais, M. Le Tacon, D. Colson, and A. Forget, Phys. Rev. Lett. **101**, 097003 (2008).
[11] K. K. Gomes, A. Pasupathy, A. N. Pushp, S. Ono, Y. Ando, and A. Yazdani, Nature (London) **447**, 569 (2007).
[12] A. Pasupathy, A. Pushp, K. Gomes, C. Parker, J. Wen, Z. Zu, G. Gu, S. Ono, Y. Ando, and A. Yazdani, Science **320**, 196 (2008).

[13] Y. Kohsaka, C. Taylor, P. Wahl, A. Schmidt, J. Lee, K. Fujita, J. Alldredge, K. McElroy, J. Lee, H. Eisaki, S. Uchida, D.-H. Lee, and J. C. Davis, Nature (London) **454**, 1072 (2008).
[14] M. C. Boyer, W. D. Wise, K. Chatterjee, M. Yi, T. Kondo, T. Takeuchi, H. Ikuta, and E. W. Hudson, Nat. Phys. **3**, 802 (2007).
[15] R. Damascelli, Z. Hussain, and Z.-X. Shen, Rev. Mod. Phys. **75**, 473 (2003).
[16] J. C. Campuzano, M. R. Norman, and M. Randeria, *Physics of Superconductors* (Springer-Verlag, Springer, Berlin, 2004), Vol. II, pp. 167–273.
[17] Q. J. Chen, J. Stajic, S. N. Tan, and K. Levin, Phys. Rep. **412**, 1 (2005).
[18] P. A. Lee, N. Nagaosa, and X. G. Wen, Rev. Mod. Phys. **78**, 17 (2006).
[19] V. J. Emery and S. A. Kivelson, Nature (London) **374**, 434 (1995).
[20] P. W. Anderson, P. A. Lee, M. Randeria, T. M. Rice, N. Trivedi, and F. C. Zhang, J. Phys.: Condens. Matter **16**, R755 (2004).
[21] A. J. Leggett, Nat. Phys. **2**, 134 (2006).
[22] Q. J. Chen, C.-C. Chien, Y. He, and K. Levin, J. Supercond. Novel Magn. **20**, 515 (2007).
[23] Q. J. Chen, Y. He, C.-C. Chien, and K. Levin, arXiv:0810.1940 (unpublished).
[24] A. Kanigel, U. Chatterjee, M. Randeria, M. R. Norman, S. Souma, M. Shi, Z. Z. Li, H. Raffy, and J. C. Campuzano, Phys. Rev. Lett. **99**, 157001 (2007).
[25] D. M. Eagles, Phys. Rev. **186**, 456 (1969).
[26] A. J. Leggett, *Modern Trends in the Theory of Condensed Matter* (Springer-Verlag, Berlin, 1980), pp. 13–27.
[27] K. Levin, Q. J. Chen, C.-C. Chien, and Y. He, arXiv:0810.1938 (unpublished).
[28] S. Tan and K. Levin, Phys. Rev. B **69**, 064510 (2004).
[29] A. Iyengar, J. Stajic, Y. J. Kao, and K. Levin, Phys. Rev. Lett. **90**, 187003 (2003).
[30] Q. J. Chen, K. Levin, and I. Kosztin, Phys. Rev. B **63**, 184519 (2001).
[31] M. R. Norman, A. Kanigel, M. Randeria, U. Chatterjee, and J. C. Campuzano, Phys. Rev. B **76**, 174501 (2007).
[32] Q. J. Chen and K. Levin, Phys. Rev. B **78**, 020513(R) (2008).
[33] I. Kosztin, Q. J. Chen, B. Jankó, and K. Levin, Phys. Rev. B **58**, R5936 (1998).
[34] Q. J. Chen, I. Kosztin, B. Jankó, and K. Levin, Phys. Rev. B **59**, 7083 (1999).
[35] P. Nozières and S. Schmitt-Rink, J. Low Temp. Phys. **59**, 195 (1985).
[36] Q. J. Chen, I. Kosztin, B. Jankó, and K. Levin, Phys. Rev. Lett. **81**, 4708 (1998).
[37] J. Maly, B. Jankó, and K. Levin, Physica C **321**, 113 (1999).
[38] Y. He, C.-C. Chien, Q. J. Chen, and K. Levin, Phys. Rev. B **76**, 224516 (2007).
[39] B. Jankó, J. Maly, and K. Levin, Phys. Rev. B **56**, R11407 (1997).
[40] M. R. Norman, M. Randeria, H. Ding, and J. C. Campuzano, Phys. Rev. B **57**, R11093 (1998).
[41] A. V. Chubukov, M. R. Norman, A. J. Millis, and E. Abrahams, Phys. Rev. B **76**, 180501(R) (2007).
[42] J. Maly, B. Jankó, and K. Levin, Phys. Rev. B **59**, 1354 (1999).
[43] J. Stajic, A. Iyengar, Q. J. Chen, and K. Levin, Phys. Rev. B **68**, 174517 (2003).
[44] A. Pushp, C. V. Parker, A. N. Pasupathy, K. K. Gomes, S. Ono, J. Wen, Z. Xu, G. Gu, and A. Yazdani, arXiv: 0906.0817, Science (to be published).